Transcriptional regulator PRDM12 is essential for human pain perception

Ya-Chun Chen[1+], Michaela Auer-Grumbach[2+], Shinya Matsukawa[3], Manuela Zitzelsberger[4], Andreas C. Themistocleous[5], Tim M. Strom[6,7], Chrysanthi Samara[8], Adrian W. Moore[9], Lily Ting-Yin Cho[10], Gareth T. Young[10], Caecilia Weiss[4], Maria Schabhüttl[2], Rolf Stucka[4], Annina B. Schmid[5], Yesim Parman[11], Luitgard Graul-Neumann[12], Wolfram Heinritz[13,14], Eberhard Passarge[14,15], Rosemarie M. Watson[16], Jens Michael Hertz[17], Ute Moog[18], Manuela Baumgartner[19], Enza Maria Valente[20], Diego Pereira[21], Carlos M. Restrepo[22], Istvan Katona[23], Marina Dusl[4], Claudia Stendel[4], Thomas Wieland[6], Faye Stafford[1], Frank Reimann[24], Katja von Au[25], Christian Finke[26], Patrick J. Willems[27], Michael S. Nahorski[1], Samiha S. Shaikh[1], Ofelia Cardvahlo[1], Adeline Nicholas[1], Maeve A. McAleer[16], Maria Roberta Cilio[28], John C. McHugh[29], Sinead M. Murphy[30], Alan D. Irvine[16,31], Uffe Birk Jensen[32], Reinhard Windhager[2], Joachim Weis[23], Carsten Bergmann[33,34], Bernd Rautenstrauss[4,35], Jonathan Baets[36,37], Peter De Jonghe[36,37], Mary M. Reilly[38], Regina Kropatsch[39], Ingo Kurth[40], Roman Chrast[8,41], Tatsuo Michiue[3], David L. H. Bennett[5], C. Geoffrey Woods[1#], and Jan Senderek[4#]

[1] Department of Medical Genetics and Cambridge Institute for Medical Research, University of Cambridge, Cambridge, UK

[2] Department of Orthopaedics, Medical University Vienna, Vienna, Austria

[3] Department of Life Sciences, Graduate School of Arts and Sciences, University of Tokyo, Tokyo, Japan

[4] Friedrich-Baur-Institute, Ludwig Maximilians University Munich, Munich, Germany

[5] Nuffield Department of Clinical Neuroscience, University of Oxford, Oxford, UK

[6] Institute for Human Genetics, Helmholtz Zentrum, Neuherberg, Germany

[7] Institute of Human Genetics, Technische Universität München, Munich, Germany

[8] Department of Medical Genetics, University of Lausanne, Lausanne, Switzerland

[9] Disease Mechanism Research Core, RIKEN Brain Science Institute, Saitama, Japan

[10] Neusentis Research Unit, Pfizer, Cambridge, UK

[11] Department of Neurology, Istanbul University, Istanbul, Turkey

[12] Ambulantes Gesundheitszentrum der Charité Campus Virchow (Humangenetik), Universitätsmedizin Berlin, Berlin, Germany

[13] Praxis für Humangenetik Cottbus, Cottbus, Germany

[14] Institut für Humangenetik, Universitätsklinikum Leipzig, Leipzig, Germany

[15] Institut für Humangenetik, Universitätsklinikum Essen, Essen, Germany

[16] Department of Dermatology, Our Lady's Children's Hospital, Dublin, Ireland

[17] Department of Clinical Genetics, Odense University Hospital, Odense, Denmark
[18] Institute of Human Genetics, Heidelberg University, Heidelberg, Germany
[19] Department of Paediatrics, Hospital Barmherzige Schwestern, Linz, Austria
[20] Neurogenetics Unit, Casa Sollievo della Sofferenza, San Giovanni Rotondo, Italy
[21] Departamento de Cirugía Plástica, Hospital Infantil Universitario de San José, Bogotá, Colombia
[22] Unidad de Genética, Universidad del Rosario, Bogotá, Colombia
[23] Institut für Neuropathologie, Klinikum der RWTH Aachen, Aachen, Germany
[24] Department of Clinical Biochemistry, University of Cambridge, Cambridge, UK
[25] SPZ Neuropädiatrie Charité, Universitätsmedizin Berlin, Berlin, Germany
[26] CharitéCentrum für Zahn-, Mund- und Kieferheilkunde, Universitätsmedizin Berlin, Berlin, Germany
[27] GENDIA (GENetic DIAgnostic Network), Antwerp, Belgium
[28] Departments of Neurology and Pediatrics, University of California San Francisco, San Francisco, USA
[29] Department of Neurology and Neurophysiology, Our Lady's Children's Hospital, Dublin, Ireland
[30] Department of Neurology, Adelaide & Meath Hospital and Academic Unit of Neurology, Trinity College, Dublin, Ireland
[31] Clinical Medicine, Trinity College, Dublin, Ireland
[32] Department of Clinical Genetics, Aarhus University Hospital, Aarhus, Denmark
[33] Center for Human Genetics, Bioscientia, Ingelheim, Germany
[34] Department of Medicine, Renal Division, and Center for Clinical Research, Freiburg University Medical Center, Freiburg, Germany
[35] Medizinisch Genetisches Zentrum, Munich, Germany
[36] Neurogenetics Group, VIB Department of Molecular Genetics, and Laboratory of Neurogenetics, Institute Born-Bunge, University of Antwerp, Antwerp, Belgium
[37] Division of Neurology, Antwerp University Hospital (UZA), Antwerp, Belgium
[38] MRC Centre for Neuromuscular Diseases, UCL Institute of Neurology, National Hospital for Neurology, London, UK
[39] Department of Human Genetics, Ruhr-University Bochum, Bochum, Germany
[40] Institute of Human Genetics, Jena University Hospital, Jena, Germany
[41] Department of Neuroscience and Department of Clinical Neuroscience, Karolinska Institutet, Stockholm, Sweden

[+] These authors have made equal contributions to the research.

[#] Corresponding authors
C.G.W.: Tel +44 1223 767811; Fax +44 1223 331206; cw347@cam.ac.uk
J.S.: Tel +49 89 440057415; Fax +49 89 440057416; jan.senderek@med.uni-muenchen.de

Pain perception has evolved as a warning mechanism to detect tissue damage and dangerous environments[1,2]. In humans, however, undesirable, excess or chronic pain is a common and major societal burden for which medical treatments are currently suboptimal[3,4]. New therapeutic options have recently emerged from the study of individuals with "congenital insensitivity to pain" (CIP)[5,6]. We report CIP in 11 families in whom we identified 10 different homozygous mutations in the *PRDM12* gene (encoding PRDI-BF1 and RIZ homology domain-containing protein 12). PRDM proteins are a family of epigenetic regulators that control neural specification and neurogenesis[7,8]. We determined that PRDM12 is expressed in nociceptors and their progenitors and participates in sensory neuron development in *Xenopus* embryos. Moreover, CIP-associated mutants abrogate histone modification potential associated with wild type PRDM12. PRDM12 emerges as a key factor for orchestrating sensory neurogenesis and may hold promise as a novel pain therapeutics target[9,10].

We ascertained two families compatible with autosomal recessive CIP (**Fig. 1a**). Mutations in the known causative genes for CIP[11,12] and clinically similar types of Hereditary Autonomic and Sensory Neuropathies (HSAN IV, V)[13-15] were excluded. SNP-array-based autozygosity mapping in the consanguineous Family A revealed a single concordant 11.5 Mb homozygous region on chromosome 9q33.2-34.13 (**Fig. 1a**). Since this large interval contained almost 150 genes (**Supplementary Table 1**) we performed exome sequencing on the index patient of Family A and the unrelated singleton CIP patient from Family B. While exome sequencing of Family A yielded no potentially pathogenic variant in genes located in the autozygous region on chromosome 9, we observed a homozygous missense mutation in one of these positional candidate genes, *PRDM12*, in Family B (**Fig. 1a** and **Supplementary Fig. 1**). We then performed Sanger sequencing of *PRDM12* in Family A and identified a homozygous tri-nucleotide expansion of alanine codons from 12 to 19 in the terminal exon (**Fig. 1a** and **Supplementary Fig. 1**). In an independent approach, exome sequencing on two unrelated singleton families with genetically unclassified CIP, Family C and Family D (**Fig. 1b**), identified *PRDM12* as the only gene that carried different bi-allelic missense mutations in both affected individuals (**Fig. 1b** and **Supplementary Fig. 1)**. Subsequently, we screened *PRDM12* in 158 individuals with autosomal recessive or isolated unexplained CIP or HSAN. We found seven further

unrelated index patients with homozygous *PRDM12* mutations. The majority of the variants were missense mutations, however, one multi-affected family (J) had an 18-alanine repeat mutation, one singleton patient (Family E) carried a frame-shift mutation and another singleton case (Family K) had an obligatory splice-site mutation (**Fig. 1c** and **Supplementary Fig. 1**). This study was approved by the National Research Ethics Service, NRES Committee East of England - Cambridge Central, the Munich University Medical Research Ethics Committee and Medical University of Vienna Ethics Committee. Informed consent was obtained from all study subjects.

PRDM12 is a 5-exon gene encoding a single protein isoform of 367 amino acids containing a PR domain (related to the SET methyltransferase domain), three zinc fingers and a C-terminal poly-alanine tract (**Fig. 1c**). The point mutations were spread throughout the gene, altered strictly conserved protein residues and were predicted to interfere with normal protein function (**Supplementary Fig. 2**, **Supplementary Table 2** and **Supplementary Note**). In all eleven families the *PRDM12* mutations segregated as expected for recessive disease alleles (**Supplementary Fig. 1**). None of the point mutations was present in public SNP databases (1000 Genomes, Exome Variant Server, dbSNP138), and in the in-house exome datasets of the Helmholtz Zentrum München and Cambridge Biomedical Research Campus. These resources altogether allow interrogation of exome data of >20,000 individuals. We suspected that the tri-nucleotide expansions to 18 and 19 alanine codons in two of our families are deleterious as other recessive and X-linked poly-alanine expansion diseases known in man clinically manifest when the number of repeats exceeds >15[16,17]. We found that the PRDM12 poly-alanine length was polymorphic in the general population with a maximum of 14 alanines (**Fig. 1d** and **Supplementary Fig. 3**). This confirms that the Family A and Family J results are exceptional.

The phenotype in the eleven *PRDM12* families was largely consistent. Patients were unable to feel acute or inflammatory pain from birth and could not identify noxious heat or cold. Consequently, infants and children suffered from painless mutilating tongue, perioral and finger lesions due to repeated self-biting and sustained multiple injuries as the result of repeated trauma and burns that often went unnoticed (**Fig. 2a**, **Supplementary Note** and **Supplementary Table 3**). Corneal reflexes were absent which led to progressive corneal scarring. Patients suffered from repeated

infections of skin and occasionally of bones and joints. In severely affected individuals, bone deformities and neuropathic joints were complications seen later in life. Notably, large fibre sensory modalities (light touch, vibration, proprioception) were normal whenever tested. Sweating and tearing occurred but were substantially reduced. The patients had no further evidence of autonomic dysfunction and sense of smell and hearing were normal. One family (J) had a milder phenotype with facial scratching, diabetes-like foot ulcers, and intact corneal reflexes, sweating and tearing. Heterozygote carriers were all asymptomatic and had normal pain perception. We studied nerve biopsies of CIP patients, done for diagnostic purposes several years ago, to evaluate peripheral projections of nociceptive sensory neurons (small myelinated Aδ fibres, normally innervating 30% of nociceptors, and unmyelinated C fibres, normally innervating 70% of nociceptors[18]). We observed a severe loss of Aδ fibres in the sural nerves of two patients while large calibre axons for other sensory modalities were largely unaltered (**Fig. 2b**). Quantitative and qualitative changes of C fibres could not be reliably determined in the nerve biopsies (as no suitable samples for electron microscopy were available[19]). Results from skin biopsies of two CIP patients suggested that at least the peripheral terminals of C fibres are affected as we observed a complete absence of nerve fibres crossing the basement membrane to innervate the epidermis (normally representing the terminals of nociceptors and thermoceptors[18]) while the subepidermal neural plexus as well as autonomic innervation of sweat glands appeared reduced in density but were grossly normal in morphology (**Fig. 2c** and **Supplementary Fig. 4**).

Our clinical and histological findings suggest that mutations in *PRDM12* cause a specific defect during the development of sensory neurons that become nociceptors. We therefore explored the expression of *PRDM12* during mouse embryogenesis and in human pain neurons generated from stem cells. In mice, *Prdm12* expression starts around embryonic day 9.0 (E9.0) in the neural folds which give rise to neural crest cells (**Fig. 3a**). The neural crest is a transient, multipotent, migratory cell population that develops into various tissues, including sensory ganglia that contain nociceptor cell bodies[20]. *Prdm12* is prominently expressed in sensory spinal ganglia (dorsal root ganglia, DRG) but not in sympathetic ganglia during the time when sensory neurons are born (E10.5-E13.5), mature and differentiate (E14.5-P14)[21] (**Fig. 3b** and **Supplementary Fig. 5a**). In addition, we demonstrated *Prdm12* is primarily

expressed by neurons rather than satellite glial cells or Schwann cells in the DRG (**Supplementary Fig. 5b**). To assess *PRDM12* expression during nociceptor development in human we differentiated inducible pluripotent stem cells (iPSCs) into nociceptor-like neurons[22,23]. *PRDM12* expression began to increase from day 7 commensurate with neural crest specification. Expression thence increased by more than 1,000 fold and peaked at day 9 (**Fig. 3c**). We further examined the electrophysiological properties of these cells after neuronal maturation, and confirmed recording of nociceptor-specific tetrodotoxin-resistant sodium current (**Supplementary Fig. 6a,b**). In addition, human embryonic stem cells (hESCs)-differentiated nociceptor-like neurons also showed a robust induction of *PRDM12* expression during differentiation (**Supplementary Fig. 6c**). We also examined *PRDM12* expression in human adult tissues and found no expression in any of these tissues except DRG (**Supplementary Fig. 7**). Taken together these findings are in accord with an essential function for PRDM12 during nociceptor neurogenesis (although we note that limited expression of *PRDM12* has been observed in mice brain and in mice and zebrafish spinal cord[8,24]). A role of PRDM12 in neural embryogenesis is further supported by the study of *Xenopus Prdm12* morphants. The knockdown resulted in irregular distribution of marker genes of cranial sensory placodes[25] at late tailbud stage (stage 28) (**Fig. 3d**, **Supplementary Fig. 8**) suggesting PRDM12 is a universal vertebrate regulator of sensory neurogenesis.

We next investigated the consequences of CIP-associated mutations on PRDM12 protein function. PRDM12 is a nuclear protein with a diffuse, lace-like pattern. The missense mutations neither affect subcellular localisation nor protein expression, however the poly-alanine expansion mutation formed discrete, concentrated foci in the nucleus and cytoplasm and resulted in reduced levels of overexpressed PRDM12 in transfected cells (**Fig. 4a** and **Supplementary Fig. 9a,b**). Expression levels of the poly-alanine expansion mutant were recovered upon proteasome inhibition (**Fig. 4a**), suggesting that the expansion causes aggregation of PRDM12 and renders the protein less stable and more susceptible to proteolysis, reducing its biological availability within the nucleus. Similar observations have been reported in other human pathogenic poly-alanine expansions[16,17]. PRDM12 is a member of a family of transcriptional regulators that participate in the control of vertebrate neurogenesis[7,8,24-29]. Unlike other PRDM family members, PRDM12 lacks intrinsic

histone methyltransferase activity and recruits the methyltransferase G9a (EHMT2) to di-methylate histone H3 at position lysine 9 (H3K9me2)[30]. Histone modifications have emerged as critical epigenetic checkpoints during neurogenesis[31-34] and aberrant epigenetic mechanisms and defects in neuronal development are associated in other human diseases[35-38]. Therefore, we next investigated the effect of *PRDM12* mutations on H3K9me2. Overexpression of wild type PRDM12 robustly increased H3K9me2 in *Xenopus* neurula stage embryos while none of the CIP-associated missense PRDM12 mutants had such an effect (**Fig. 4b**). Also both wild type human and mouse PRDM12 strongly induced H3K9me2 in *Xenopus* embryos, despite that the mammalian orthologues differ by ~15% of amino acids from the frog protein. This supports impaired histone methylation capacity as the mechanism of CIP-causing *PRDM12* missense mutations (**Supplementary Fig. 10**). Mechanistically, we found that the p.His289Leu mutation significantly reduced binding to G9a, whereas the other mutants bound normally (**Fig. 4c** and **Supplementary Fig. 9d**). The putative structure of PRDM12 implies His289 is one of the residues coordinating the zinc ion of the second zinc finger (**Fig. 4c**), which is required for G9a association[30]. The mechanism through which other PRDM12 mutants interfere with H3K9 di-methylation remains to be determined (**Supplementary Fig. 9**). Mutations of Ile102 and Trp160 that are located in the core of the PR domain (**Fig. 4d**) are likely to alter the domain's structure. Arg168 and Glu172 contribute to the surface of the PR domain. Since PR domains represent protein interaction modules[39-42], mutations affecting these residues may alter protein-binding capability of PRDM12-PR.

PRDM12 is essential for pain sensing in humans as pathogenic mutations cause congenital painlessness. Our data imply that the pathological mechanism is a loss of control of histone modification during critical points in nociceptor genesis, possibly via G9a or related factors[34]. Increasingly the pathophysiology of chronic and neuropathic pain has focussed upon epigenetic changes in the peripheral and spinal cord nociceptive circuits[9,10]. The histone modifying activity of PRDM12 suggests the possibility of developing novel methods of pain relief through reprogramming overactive nociceptors into pain-free states.

Methods

Methods and associated references are available in the online version of the paper.

Acknowledgments

The authors are grateful for the participation of the patients and their families in this study. The help of all contributing medical, technical and administrative staff is greatly appreciated. We thank Dr. José Rolando Prada Madrid and Dr. Felicia Axelrod for advice and discussion. This work was supported by Cambridge NIHR BRC for Y.-C.C., F.S. and C.G.W., Austrian Science Fond (P23223-B19) for M.A.-G., UK MRC for M.S.N. and S.S.S., Deutsche Forschungsgemeinschaft (KU1587/4-1) for I. Kurth, and Gebert-Rüf Stiftung (GRS-046/09) and Friedrich-Baur Stiftung for J.S.

Author Contributions

M.A.-G., Y.P., L.G.-N., W.H., R.M.S., J.M.H., U.M., M.B., D.P., C.M.R., K.v.A., C.F., M.A.McA., J.C.McH., S.M.M., A.D.I., U.B.J., C.G.W. and J.S. took care of and enrolled patients in the study. Y.P., L.G.-N., E.P., J.M.H., E.M.V., P.J.W., M.R.C., C.B., B.R., J.B., P.D.J., M.M.R., R.K., I. Kurth and C.G.W. provided DNA samples, skin biopsies and nerve biopsy specimens. Y.-C.C., M.A.-G., T.M.S., C.W., M.S., T.W., F.S., M.S.N., S.S.S., O.C., A.N., C.G.W. and J.S. undertook linkage analysis and *PRDM12* mutation screening. Y.-C.C., M.Z., C. Samara, A.W.M., R.S. and R.C. performed expression studies on *PRDM12*. Y.-C.C., S. M., M.Z., C.W., R.S., M.D., C. Stendel, F.R., T.M. and J.S. assessed functional consequences of mutations in *PRDM12*. A.C.T., A.B.S., I. Katona, J.W. and D.L.H.B. analysed skin biopsies from CIP patients. T.M. and S. M. performed experiments in *Xenopus* embryos. Y.-C.C., L.T.-Y.C. and G.T.Y. were responsible for experiments involving pluripotent stem cells. R.S. and J.S. undertook the protein modeling. A.W.M., R.W., J.W., I. Kurth and D.L.H.B. gave critical advice. M.A.-G., C.G.W. and J.S. oversaw the project,

participated in data analysis and directed and supervised the research. The manuscript was written by Y.-C.C., M.A.-G., C.G.W. and J.S. with input from other authors.

Competing Financial Interests

The authors declare no competing financial interests.

References

1. Merskey, H. & Watson, G.D. The lateralisation of pain. *Pain* **7**, 271-280 (1979).
2. Bennett, D.L. & Woods, C.G. Painful and painless channelopathies. *Lancet Neurol.* **13**, 587-599 (2014).
3. Stewart, W.F., Ricci, J.A., Chee, E., Morganstein, D. & Lipton, R. Lost productive time and cost due to common pain conditions in the US workforce. *JAMA* **290**, 2443-2454 (2003).
4. Breivik, H., Collett, B., Ventafridda, V., Cohen, R. & Gallacher, D. Survey of chronic pain in Europe: prevalence, impact on daily life, and treatment. *Eur. J. Pain* **10**, 287-333 (2006).
5. Goldberg, Y.P. *et al.* Human Mendelian pain disorders: a key to discovery and validation of novel analgesics. *Clin. Genet.* **82**, 367-373 (2012).
6. Holmes, D. Anti-NGF painkillers back on track? *Nat. Rev. Drug. Discov.* **11**, 337-338 (2012).
7. Hohenauer, T. & Moore, A.W. The Prdm family: expanding roles in stem cells and development. *Development* **139**, 2267-2282 (2012).
8. Kinameri, E. *et al.* Prdm proto-oncogene transcription factor family expression and interaction with the Notch-Hes pathway in mouse neurogenesis. *PLoS One* **3**, e3859 (2008).
9. Crow, M., Denk, F. & McMahon, S.B. Genes and epigenetic processes as prospective pain targets. *Genome Med.* **5**, 12 (2013).
10. Denk, F. & McMahon, S.B. Chronic pain: emerging evidence for the involvement of epigenetics. *Neuron* **73**, 435-444 (2012).

11. Cox, J.J. *et al.* An SCN9A channelopathy causes congenital inability to experience pain. *Nature* **444**, 894-898 (2006).

12. Leipold., E. *et al.* A de novo gain-of-function mutation in SCN11A causes loss of pain perception. *Nat. Genet.* **45**, 1399-1404 (2013).

13. Indo, Y. *et al.* Mutations in the TRKA/NGF receptor gene in patients with congenital insensitivity to pain with anhidrosis. *Nat. Genet.* **13**, 485-488 (1996).

14. Einarsdottir, E. *et al.* A mutation in the nerve growth factor beta gene (NGFB) causes loss of pain perception. *Hum. Mol. Genet.* **13**, 799-805 (2004).

15. Carvalho, O.P. *et al.* A novel NGF mutation clarifies the molecular mechanism and extends the phenotypic spectrum of the HSAN5 neuropathy. *J. Med. Genet.* **48**, 131-135 (2011).

16. Albrecht, A. & Mundlos, S. The other trinucleotide repeat: polyalanine expansion disorders. *Curr. Opin. Genet. Dev.* **15**, 285-293 (2005).

17. Hughes, J. *et al.* Mechanistic insight into the pathology of polyalanine expansion disorders revealed by a mouse model for X linked hypopituitarism. *PLoS Genet.* **9**, e1003290 (2013).

18. Dubin, A.E. & Patapoutian, A. Nociceptors: the sensors of the pain pathway. *J. Clin. Invest.* **120**, 3760-3772 (2010).

19. Ochoa, J. & Mair, W.G. The normal sural nerve in man. I. Ultrastructure and numbers of fibres and cells. *Acta Neuropathol.* **13**, 197-216 (1969).

20. Hall, B.K. The neural crest and neural crest cells: discovery and significance for theories of embryonic organization. *J. Biosci.* **33**, 781-793 (2008).

21. Ma, Q., Fode, C., Guillemot, F. & Anderson, D.J. Neurogenin1 and neurogenin2 control two distinct waves of neurogenesis in developing dorsal root ganglia. *Genes Dev.* **13**, 1717-1728 (1999).

22. Chambers, S.M. *et al.* Combined small-molecule inhibition accelerates developmental timing and converts human pluripotent stem cells into nociceptors. *Nat. Biotechnol.* **30**, 715-720 (2012).

23. Young, G.T. *et al.* Characterizing human stem cell-derived sensory neurons at the single-cell level reveals their ion channel expression and utility in pain research. *Mol. Ther.* **22**, 1530-1543 (2014).

24. Zannino, D.A., Downes, G.B. & Sagerström, C.G. Prdm12b specifies the p1 progenitor domain and reveals a role for V1 interneurons in swim movements. *Dev. Biol.* **390**, 247-260 (2014).

25. Schlosser., G. Induction and specification of cranial placodes. *Dev. Biol.* **294**, 303-351 (2006).

26. Moore, A.W., Jan, L.Y. & Jan, Y.N. Hamlet, a binary genetic switch between single- and multiple- dendrite neuron morphology. *Science* **297**, 1355-1358 (2002).

27. Rossi, C.C., Kaji, T. & Artinger, K.B. Transcriptional control of Rohon-Beard sensory neuron development at the neural plate border. *Dev. Dyn.* **238**, 931-943 (2009).

28. Endo, K. *et al.* Chromatin modification of Notch targets in olfactory receptor neuron diversification. *Nat. Neurosci.* **15**, 224-233 (2011).

29. Chittka, A., Nitarska, J., Grazini, U. & Richardson, W.D. Transcription factor positive regulatory domain 4 (PRDM4) recruits protein arginine methyltransferase 5 (PRMT5) to mediate histone arginine methylation and control neural stem cell proliferation and differentiation. *J. Biol. Chem.* **287**, 2995-3006 (2012).

30. Yang, C.M. & Shinkai, Y. Prdm12 is induced by retinoic acid and exhibits anti-proliferative properties through the cell cycle modulation of P19 embryonic carcinoma cells. *Cell. Struct. Funct.* **38**, 195-204 (2013).

31. Hu, X.L., Wang, Y. & Shen, Q. Epigenetic control on cell fate choice in neural stem cells. *Protein & Cell* **3**, 278-290 (2012).

32. Tan, S.L. *et al.* Essential roles of the histone methyltransferase ESET in the epigenetic control of neural progenitor cells during development. *Development* **139**, 3806-3816 (2012).

33. Jobe, E.M., McQuate, A.L. & Zhao, X. Crosstalk among epigenetic pathways regulates neurogenesis. *Front. Neurosci.* **6**, 59 (2012).

34. Boshnjaku, V. *et al.* Epigenetic regulation of sensory neurogenesis in the dorsal root ganglion cell line ND7 by folic acid. *Epigenetics* **6**, 1207-1216 (2011).

35. Amir, R.E. *et al.* Rett syndrome is caused by mutations in X-linked MECP2, encoding methyl-CpG-binding protein 2. *Nat. Genet.* **23**, 185-188 (1999).

36. Kleefstra, T. *et al.* H. Loss-of-function mutations in euchromatin histone methyl transferase 1 (EHMT1) cause the 9q34 subtelomeric deletion syndrome. *Am. J. Hum. Genet.* **79**, 370-377 (2006).

37. Klein, C.J. *et al.* Mutations in DNMT1 cause hereditary sensory neuropathy with dementia and hearing loss. *Nat. Genet.* **43**, 595-600 (2011).

38. Jakovcevski, M. & Akbarian, S. Epigenetic mechanisms in neurological disease. *Nat. Med.* **18**, 1194-1204 (2012).

39. Huang, S., Shao, G. & Liu, L. The PR domain of the Rb-binding zinc finger protein RIZ1 is a protein binding interface and is related to the SET domain functioning in chromatin-mediated gene expression. *J. Biol. Chem.* **273**, 15933-15939 (1998).

40. Rozenblatt-Rosen, O. *et al.* The C-terminal SET domains of ALL-1 and TRITHORAX interact with the INI1 and SNR1 proteins, components of the SWI/SNF complex. *Proc. Natl. Acad. Sci. U. S. A.* **95**, 4152-4157 (1998).

41. Cui, X. *et al.* Association of SET domain and myotubularin-related proteins modulates growth control. *Nat. Genet.* **18**, 331-337 (1998).

42. Cardoso, C. *et al.* Specific interaction between the XNP/ATR-X gene product and the SET domain of the human EZH2 protein. *Hum. Mol. Genet.* **7**, 679-684 (1998).

Figure Legends

Figure 1 Identification of mutations in *PRDM12*. (**a**) In Pakistani multiplex Family A, SNP-based autozygosity mapping of four individuals (filled red circles) pinpointed a single candidate region on chromosome 9q33.2-34.13 (represented by rs-numbers of flanking SNP markers and a red bar next to the chromosome 9 ideogram). While exome sequencing of the index patient from Family A (open blue circle) yielded inconclusive results, one gene in the candidate region, *PRDM12*, harboured a candidate homozygous mutation in singleton Family B (filled blue circle). (**b**) Exome sequencing of patients from two singleton CIP-families, Family C and Family D (filled blue circles). *PRDM12* was the only gene containing serious variants excluded from all databases (DB) on both alleles (AR model) in both affected individuals (Shared). (**c**) Schematic representation of the PRDM12 protein and distribution of mutations. Amino acid numbering is shown below. PR: PR domain; ZF: zinc finger motif. (**d**) Distribution of PRDM12 poly-alanine tract lengths within the general population (176 individuals).

Figure 2 Phenotype of patients with *PRDM12* mutations. (**a**) Mutilations of tongue and lips, corneal opacity, scaring and mutilations of distal phalanges. Patients P17 and P18 (Family J) represent a milder phenotype with sequelae of facial scratching and diabetes-like foot ulcer. Consent to publish images of the individuals was obtained. (**b**) Sural nerve biopsy specimens revealing selective loss of small calibre myelinated axons. Total number of myelinated fibres per area (1/mm^2) was 4,692 (P6), 4,438 (P10) and 9,609 (healthy control). Semithin sections, toluidine blue staining; scale bars: 20 µm. (**c**) Skin biopsies stained with pan-neuronal marker PGP9.5, CGRP (labelling a subpopulation of nociceptive primary afferents) and VIP (autonomic nerve fibre marker). While ample intraepidermal nerve endings (red

arrowheads) were observed in the biopsy from a healthy donor, nerve fibres did not cross the dermal-epidermal border (red dotted line) in the patient's biopsy. Dermal CGRP immunoreactive nerve fibres were almost absent. Sweat glands were innervated by VIP immunoreactive fibres but at reduced density. Scale bars: 50 µm (two upper rows); 20 µm (third row).

Figure 3 A role for *PRDM12* in sensory neuron development. (**a**) Whole-mount *in situ* hybridisation of mouse embryos revealed early expression of *Prdm12* in neural folds at E9.0 (filled arrowhead) which coincided with the earliest stage of neural crest cell delamination and migration (open arrowhead). Strong expression was observed in DRG at E10.5 (arrowheads). *In situ* hybridisation in a transverse spinal cord cervical section at E10.5 showed prominent *Prdm12* expression in DRG. (**b**) RT-PCR analysis confirmed *Prdm12* mRNA expression throughout the whole period of DRG development and sensory neuron differentiation (E9.5-P14) and in mature DRG (P56). (**c**) IPSC-derived sensory neurons express *PRDM12* during neural crest specification. The iPSC differentiation generated cells expressing canonical markers of sensory neurons. The pluripotency markers reduced as cells underwent differentiation. *PRDM12* expression was found to peak during neural crest specification (days 8-9). The schematic diagram illustrates the stages of development during the sensory neuron differentiation process. (**d**) Knockdown of PRDM12 by specific morpholino (Prdm12 MO) in *Xenopus* embryos causes irregular staining for markers of cranial sensory placode development, *Ath3*, *EBF3* and *Islet1*. Embryos injected with Control MO or Prdm12 MO were analyzed at late tailbud stage (stage 28) by whole-mount *in situ* hybridisation, yellow arrowhead: profundal placode, green arrowhead: trigeminal placode. Normal gene expression domains of cranial placodes (colored outlines) in *Xenopus laevis* are shown in the schematic drawing above (lateral view, late tailbud stage, modified from[25]). The results were categorized and quantified ($n \geq 46$ alive embryos per condition). Statistical differences between Control MO- and Prdm12 MO-treated embryos are indicated: *** $P < 0.001$ (two-sided Mann-Whitney *U* test).

Figure 4 Functional characterisation of PRDM12 mutants. (**a**) Human HA-PRDM12 poly-alanine expansion mutant protein showed lower expression levels in COS-7 cells than the wild-type (quantified by normalising PRDM12 signals to α-tubulin and

GFP (transfection efficiency control)), and that was recovered upon MG132 treatment. The transfected mutant also formed aggregates in the nucleus and cytoplasm in HEK-293T cells. (**b**) Animal cap cells from *Xenopus* embryos were co-microinjected with *Myc-Prdm12* (wild type and mutants), *Wnt8* and *Chordin* mRNA and cultured until mid-neurula stage (stage 15). Wild-type PRDM12 induced robust di-methylation on H3K9 but CIP-associated missense mutants were functionless. (**c**) Myc-PRDM12 and FLAG-G9a were expressed in COS-7 cells (Input) and immunoprecipitated using anti-Myc antibody (IP: Myc). Compared to wild type PRDM12, the p.His289Leu mutation interferes with the PRDM12-G9a interaction. PRDM12 ΔZF is an artificial mutant lacking zinc fingers and served as a control. For quantification, bound G9a was normalised to PRDM12 protein amount in the IP fraction and the G9a protein amount in the cell lysate. The structural model for the PRDM12 zinc finger domains suggested that His289 (orange) is one of the residues (cyan) that coordinate the zinc ion. (**d**) Mutation-altered residues Ile102 and Trp160 (orange) in the PRDM12-PR domain are located in the core of the protein where they make hydrophobic interactions with other residues, sidechains shown in cyan. Introduction of a polar side-chain (p.Ile102Asn) or a disulfide bond partner (p.Trp160Cys) into the hydrophobic core is expected to affect the structure of the PR domain. The graphs in (a), (b) and (c) represent mean values of *n* independent experiments (biological replicates), and error bars represent SD. Statistical differences between control (wild type) and PRDM12 mutants are indicated: ns, not significant; * $P < 0.05$; ** $P < 0.01$; *** $P < 0.001$ (Welch's *t*-test).

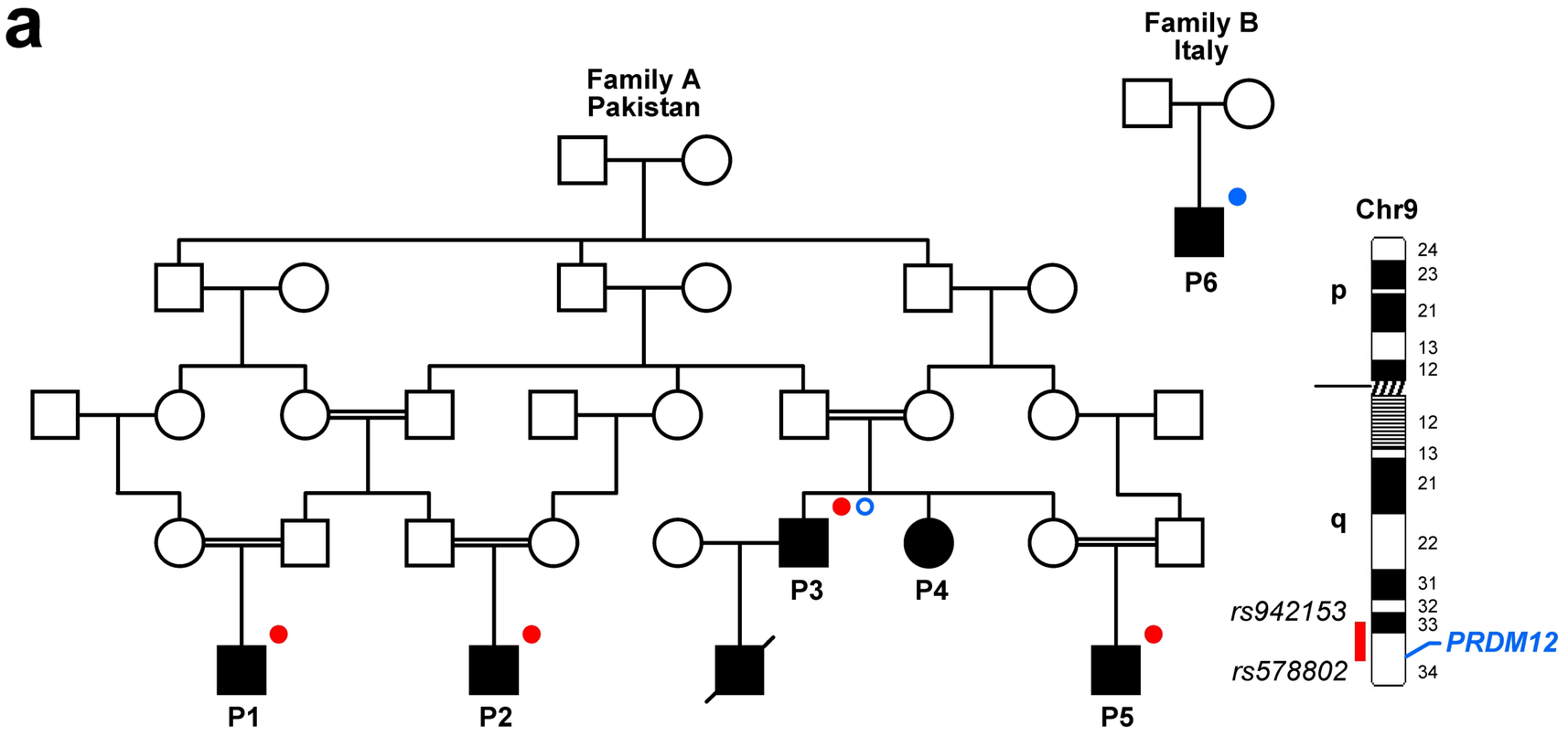

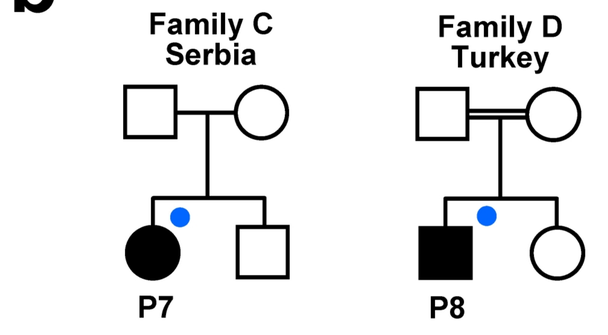

	Not in DB	AR model (genes)	Shared
P7	397	23	*PRDM12*
P8	452	37	

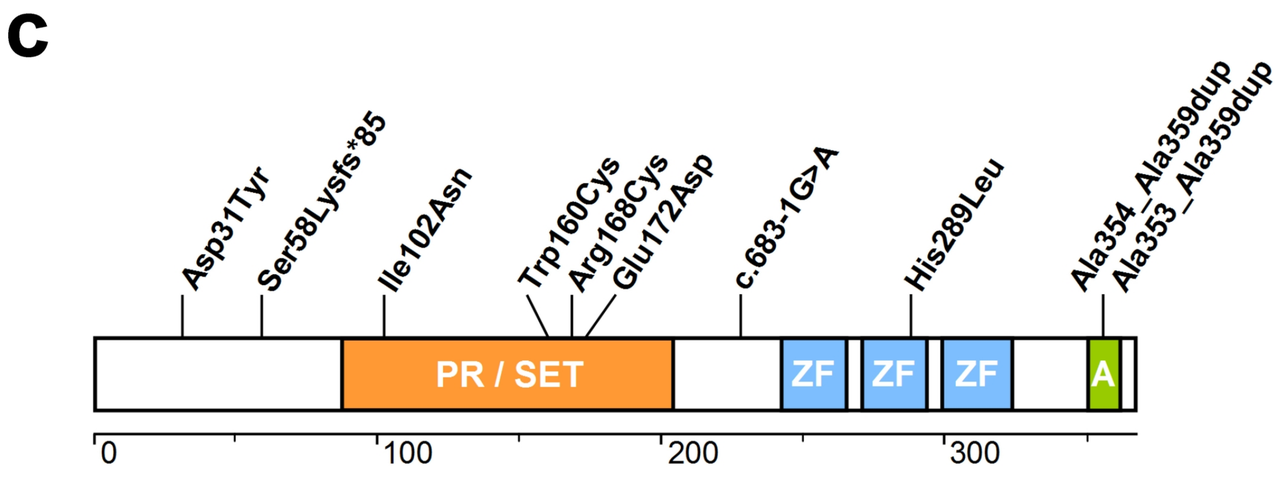

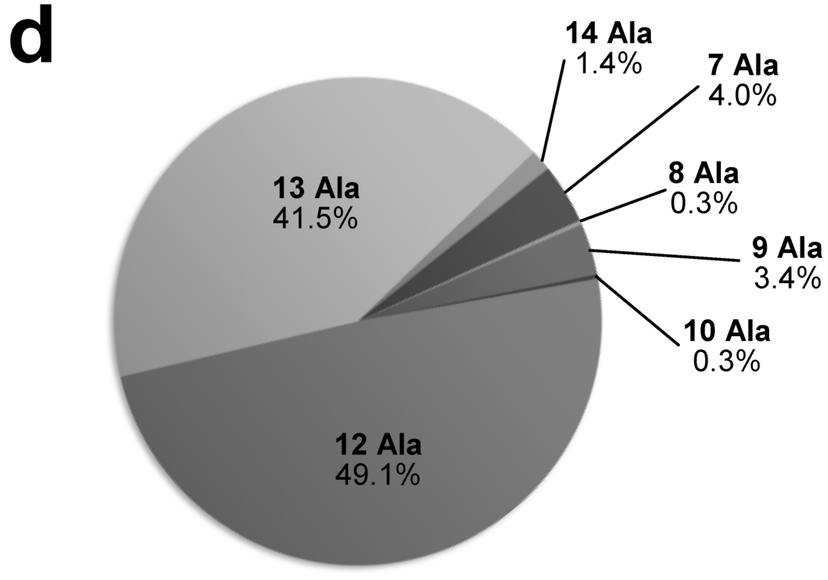

Figure 1

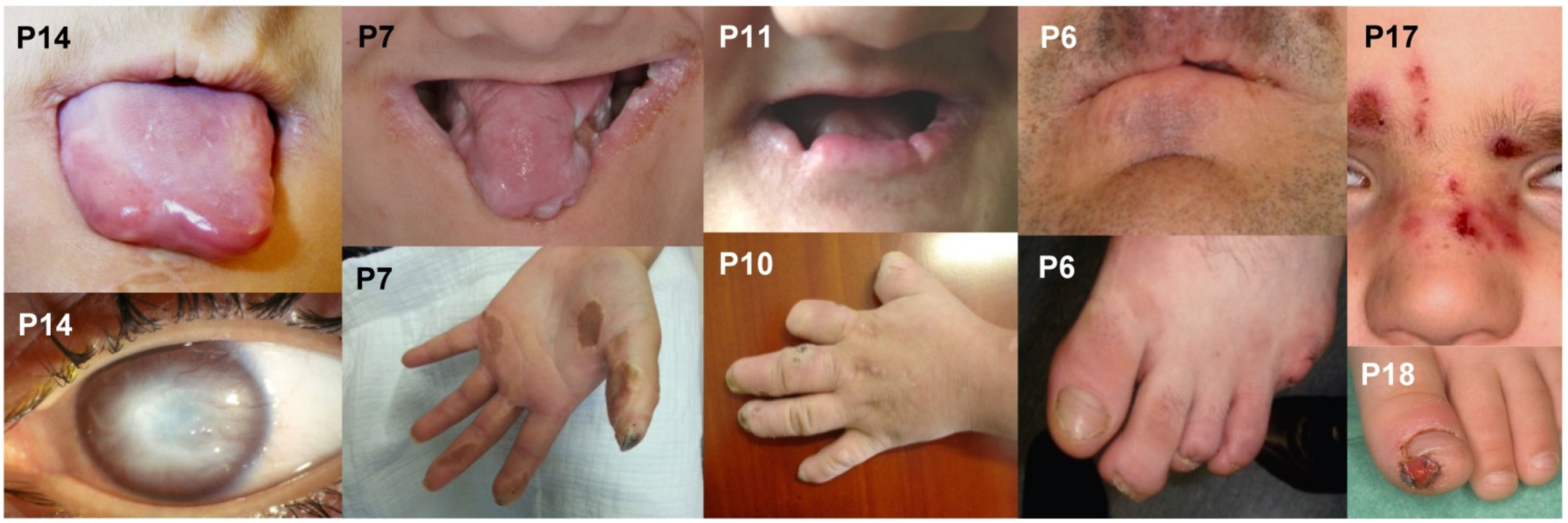
a
P14
P7
P11
P6
P17
P14
P7
P10
P6
P18
b
P6
P10
Healthy control
P6
P10
Healthy control
Myelinated fibres (n/mm²)
2000
1500
1000
500
0
1 2 3 4 5 6 7 8 9 10 11 12 13 14 15 16 17
Diameter of myelinated fibres (µm)
c
Healthy control
P11
PGP9.5
CGRP/PGP9.5
PGP9.5/VIP/DAPI

Figure 2

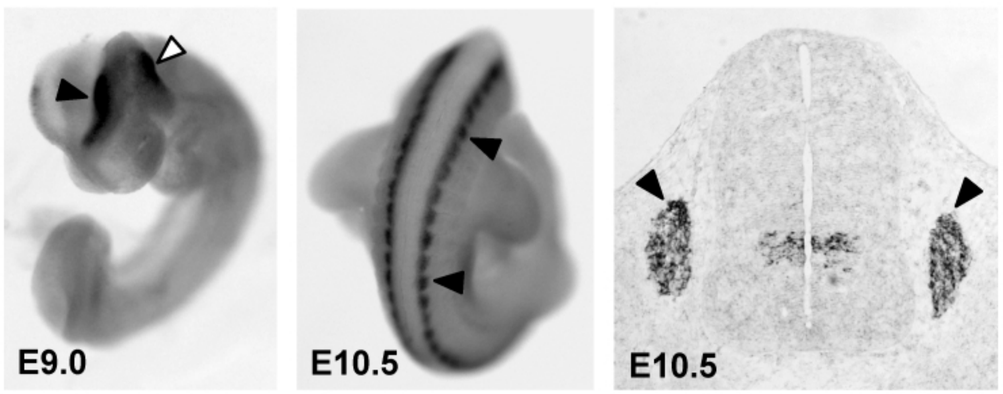
a
E9.0
E10.5
E10.5

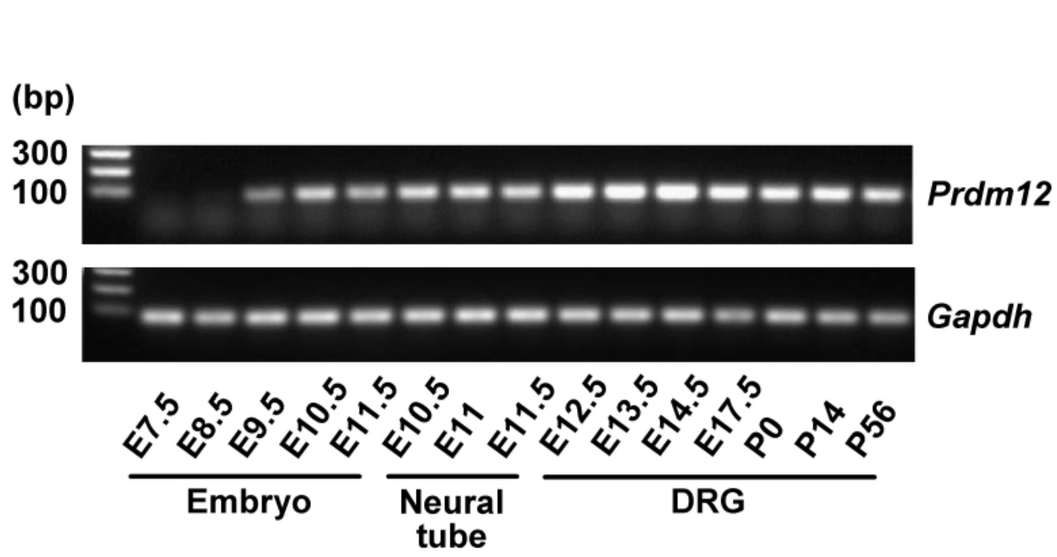
b
(bp)
300
100
Prdm12
300
100
Gapdh
E7.5
E8.5
E9.5
E10.5
E11.5
E10.5
E11
E11.5
E12.5
E13.5
E14.5
E17.5
P0
P14
P56
Embryo
Neural tube
DRG

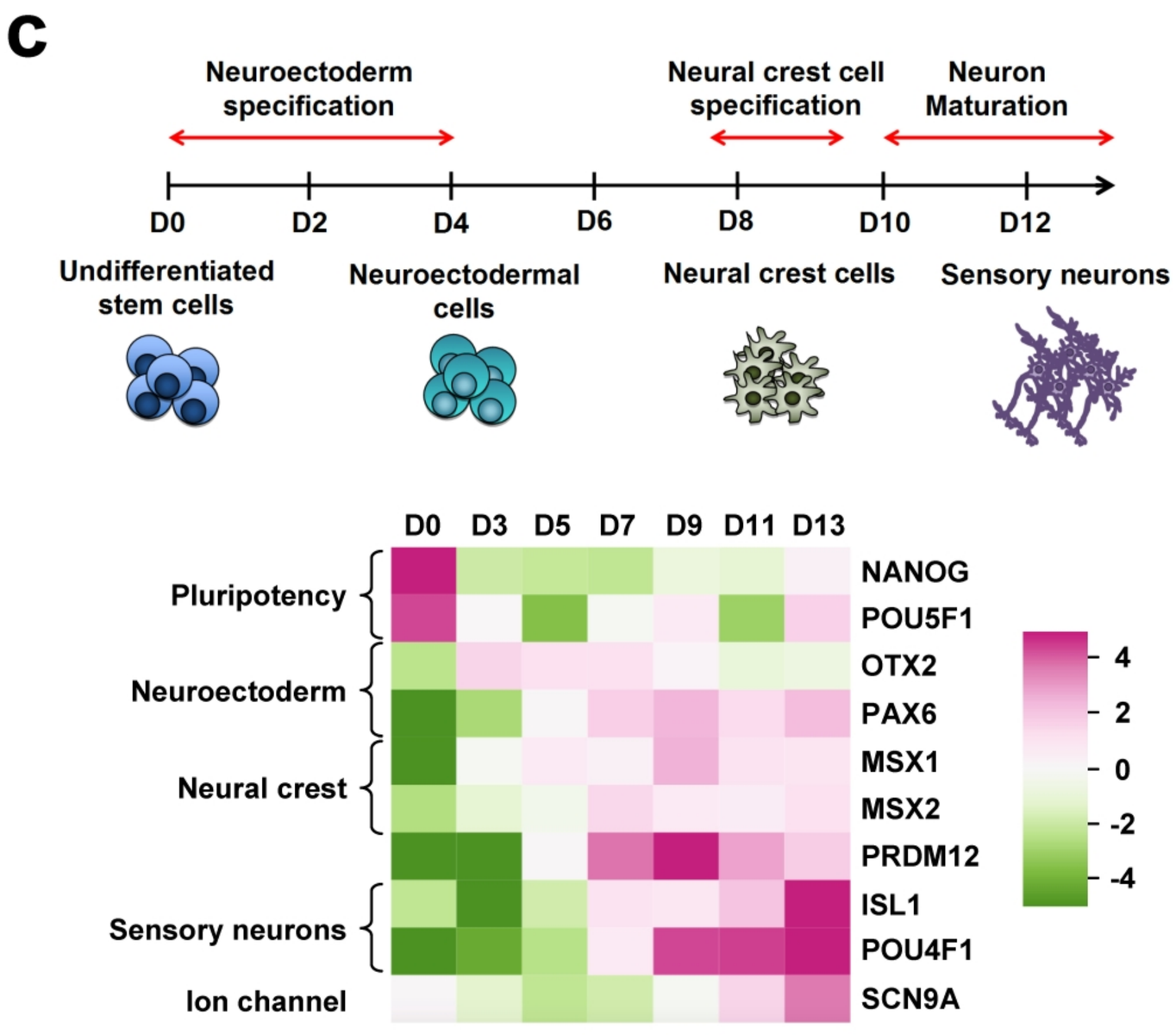
c
Neuroectoderm specification
Neural crest cell specification
Neuron Maturation
D0
D2
D4
D6
D8
D10
D12
Undifferentiated stem cells
Neuroectodermal cells
Neural crest cells
Sensory neurons
D0
D3
D5
D7
D9
D11
D13
Pluripotency
Neuroectoderm
Neural crest
Sensory neurons
Ion channel
NANOG
POU5F1
OTX2
PAX6
MSX1
MSX2
PRDM12
ISL1
POU4F1
SCN9A
4
2
0
-2
-4

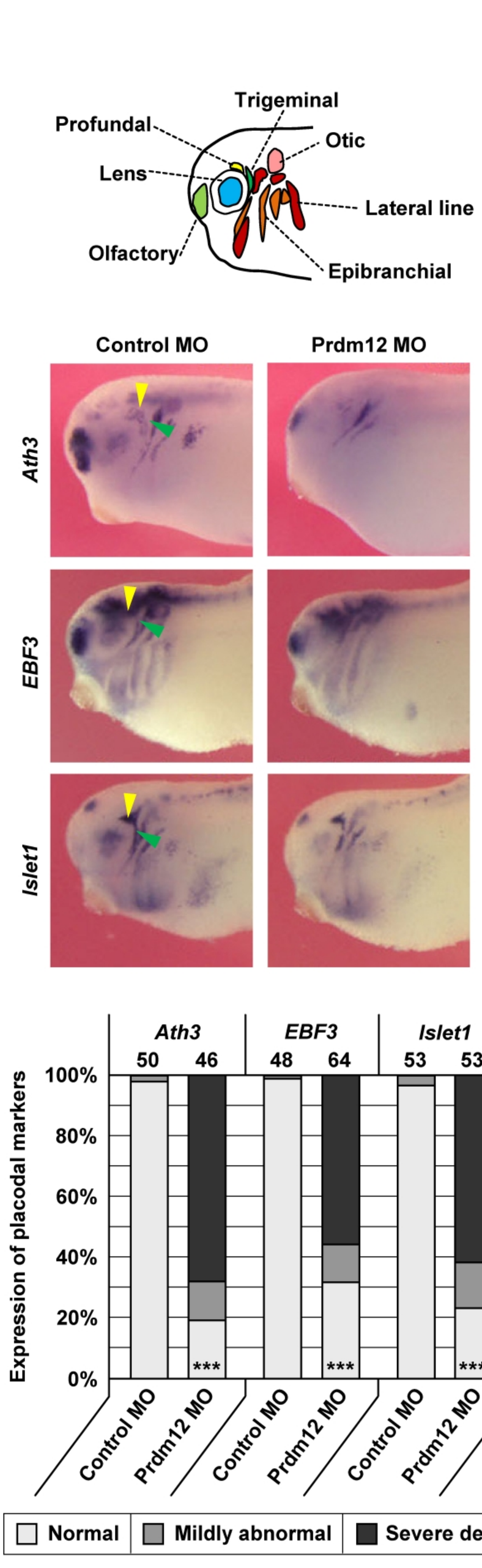
d
Trigeminal
Profundal
Otic
Lens
Lateral line
Olfactory
Epibranchial
Control MO
Prdm12 MO
Ath3
EBF3
Islet1
Ath3
EBF3
Islet1
50
46
48
64
53
53
n
Expression of placodal markers
100%
80%
60%
40%
20%
0%
***
***
***
Control MO
Prdm12 MO
Control MO
Prdm12 MO
Control MO
Prdm12 MO
Normal
Mildly abnormal
Severe defects

Figure 3

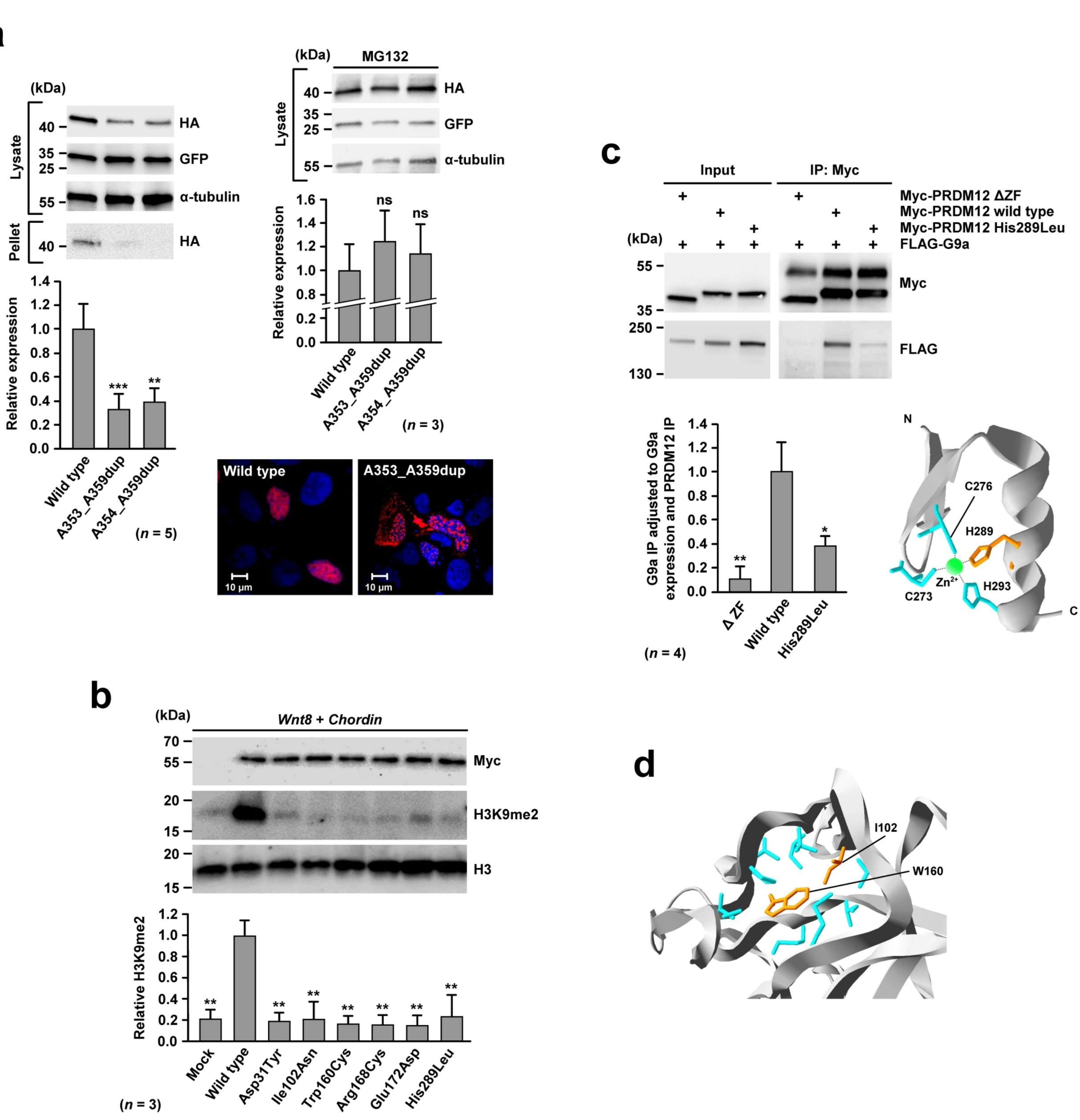
a
(kDa)
Lysate
40
35
25
55
HA
GFP
α-tubulin
Pellet
40
HA
Relative expression
1.4
1.2
1.0
0.8
0.6
0.4
0.2
0.0
***
**
Wild type
A353_A359dup
A354_A359dup
(n = 5)
(kDa)
MG132
Lysate
40
35
25
55
HA
GFP
α-tubulin
Relative expression
1.6
1.4
1.2
1.0
0.8
0.2
0.0
ns
ns
Wild type
A353_A359dup
A354_A359dup
(n = 3)
Wild type
A353_A359dup
10 μm
10 μm
c
Input
IP: Myc
Myc-PRDM12 ΔZF
Myc-PRDM12 wild type
Myc-PRDM12 His289Leu
FLAG-G9a
(kDa)
55
35
250
130
Myc
FLAG
G9a IP adjusted to G9a expression and PRDM12 IP
1.4
1.2
1.0
0.8
0.6
0.4
0.2
0.0
**
*
Δ ZF
Wild type
His289Leu
(n = 4)
N
C276
H289
Zn2+
H293
C273
C
b
(kDa)
Wnt8 + Chordin
70
55
20
15
20
15
Myc
H3K9me2
H3
Relative H3K9me2
1.2
1.0
0.8
0.6
0.4
0.2
0.0
**
Mock
Wild type
Asp31Tyr
Ile102Asn
Trp160Cys
Arg168Cys
Glu172Asp
His289Leu
(n = 3)
d
I102
W160

Figure 4